Int. J. Heat Mass Transfer. Vol. 34, No. 2, pp. 407–413, 1991
Printed in Great Britain

0017–9310/91 $3.00 + 0.00

Thermodynamics of an 'isothermal' flow: the two-dimensional turbulent jet

ADRIAN BEJAN
Department of Mechanical Engineering and Materials Science, Duke University, Durham, NC 27706, U.S.A.

(*Received* 3 *July* 1989 *and in final form* 26 *March* 1990)

Abstract—This study illustrates the thermodynamic information that is being routinely overlooked by a pure fluid mechanics analysis. The integral analysis of the two-dimensional turbulent jet is used as an example. It is shown that even when the temperature difference between the nozzle fluid and the reservoir fluid is zero, the jet region is nonisothermal. At every position along the jet, the temperature rise becomes maximum when the entrainment coefficient assumes a value that is comparable with the value determined experimentally. Furthermore, it appears that the natural shape of the velocity and temperature profiles of the jet is the one that minimizes the total entropy generation rate. This study suggests that an important relationship exists between the empirical components of the pure-fluid-mechanics integral treatment, and the temperature and entropy generation extrema unveiled by the thermodynamic analysis

INTRODUCTION

THE traditional approach in the study of fluid flows in which the transfer of heat and mass is not an issue (i.e. in 'pure' fluid mechanics) is to overlook entirely the thermodynamic analysis of the flow. The objective of the present study is to bring to light the kind of information—the thermodynamic aspect—that is being overlooked by the traditional method. This aspect serves as focus for an entire subfield in heat transfer today [1, 2]. It will be shown that an interesting relationship exists between the empirical content of the pure fluid mechanics treatment, and the temperature and entropy generation rate distributions that are revealed by the thermodynamic analysis.

The thermodynamic facet of a traditional pure-fluid-mechanics treatment can be seen by reconsidering the classical example of the two-dimensional turbulent jet. Figure 1 shows that the jet is produced by a narrow slit of width D_0, and that its slit-averaged velocity is u_0. The pressure of the fluid reservoir is uniform. At longitudinal distances x greater than a few slit widths, the time-averaged flow field is described by the velocity components u and v, which must satisfy the time-averaged mass and momentum conservation equations (see, for example, p. 283 of ref. [3]).

$$\frac{\partial u}{\partial x}+\frac{\partial v}{\partial y}=0 \tag{1}$$

$$u\frac{\partial u}{\partial x}+v\frac{\partial u}{\partial y}=\frac{\partial}{\partial y}\left[(\nu+\varepsilon_M)\frac{\partial u}{\partial y}\right]. \tag{2}$$

The jet flow region is being treated as 'slender', or of the boundary layer type ($D \ll x$): this is why the pressure gradient and longitudinal diffusion terms are absent from the momentum equation (2).

One additional equation—the entrainment hypothesis—becomes a necessity in the integral analysis of the jet flow [4]. The analysis begins with assuming a certain u-profile shape, which is labeled $f(\zeta)$

$$u=u_c f(\zeta), \quad \zeta=\frac{y}{D} \tag{3}$$

and continues with integrating equations (1) and (2) across the jet region. It can be shown that this operation yields two equations, respectively

$$\frac{\mathrm{d}}{\mathrm{d}x}(I_1 u_c D)=2(-v_\infty) \tag{4}$$

$$I_2 u_c^2 D=u_0^2 D_0 \tag{5}$$

in which the centerline velocity $u_c(x)$, the jet thickness

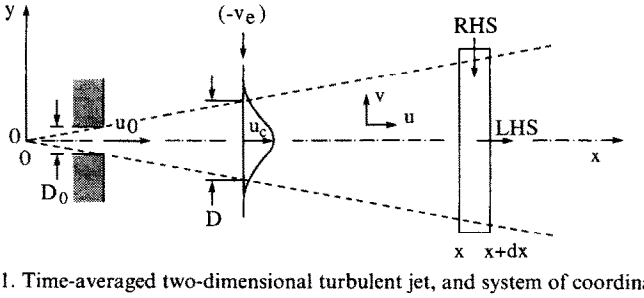

FIG. 1. Time-averaged two-dimensional turbulent jet, and system of coordinates.

NOMENCLATURE

c	specific heat of incompressible liquid
c_p	specific heat at constant pressure
D	transversal length scale of jet flow region
D_0	nozzle spacing size (Fig. 1)
f	velocity and temperature profile shape, equations (3) and (18)
h	specific enthalpy, time averaged
h_∞	specific enthalpy of reservoir fluid
I_1, I_2, I_3	definite integrals, equations (6) and (21)
s	specific entropy, time averaged
s_∞	specific entropy of reservoir fluid
S_{gen}	entropy generation rate in finite-length jet region, equation (28)
T	time-averaged temperature
T_c	centerline temperature
ΔT_c	centerline temperature rise, $T_c - T_\infty$
T_∞	temperature of reservoir fluid
u	time-averaged longitudinal velocity
u_c	centerline velocity
u_0	longitudinal velocity through the nozzle
v	time-averaged transversal velocity
$-v_\infty$	entrainment velocity
x	longitudinal coordinate
y	transversal coordinate.

Greek symbols

α	entrainment coefficient, equation (7)
α_c	empirical entrainment coefficient, equation (15)
α_{opt}	optimum entrainment coefficient, equation (23)
γ	empirical constant, equation (13)
ε_M	momentum eddy diffusivity
ζ	dimensionless transversal coordinate, y/D
ν	kinematic viscosity
ρ	density.

Superscripts and subscripts

$(\tilde{\ })$	dimensionless variables defined in equations (10), (20) and (28)
$(\ )_{max}$	maximum.

scale $D(x)$, and the entrainment velocity $-v_\infty(x)$ are unknown. The numerical coefficients I_1 and I_2 are shorthand for two integrals the values of which will be compared later in Table 1

$$I_1 = \int_{-\infty}^{\infty} f\,d\zeta, \quad I_2 = \int_{-\infty}^{\infty} f^2\,d\zeta. \tag{6}$$

The two-equation system, equations (4) and (5), is clearly not sufficient for determining the three unknowns uniquely. The classical way out of this difficulty is to use the entrainment hypothesis, that is, the statement that the entrainment velocity is proportional to the longitudinal velocity

$$-v_\infty = \alpha u_c \tag{7}$$

in which the entrainment coefficient α is a constant to be determined empirically. The (u_c, D) solution to equations (4) and (5) (obtained by integrating away from the virtual origin $x = 0$, where $u_c = \infty$) is

$$\tilde{u}_c = \left(\frac{I_1}{4\alpha I_2}\right)^{1/2} \tilde{x}^{-1/2} \tag{8}$$

$$\tilde{D} = \frac{4\alpha}{I_1}\tilde{x}. \tag{9}$$

The dimensionless variables used above are defined by

$$\tilde{x} = \frac{x}{D_0}, \quad \tilde{u}_c = \frac{u_c}{u_0}, \quad \tilde{D} = \frac{D}{D_0} \tag{10}$$

such that $\tilde{D} = 1$ (or $\tilde{x} = I_1/4\alpha$) represents the longi-

Table 1. The effect of the velocity and temperature profile shape on the total entropy generation rate

Profile shape	I_1	I_2	I_3	$I_3/I_2^{3/2} = \tilde{S}_{gen,max}$
Triangular, $f = 1-\lvert\zeta\rvert$, $\lvert\zeta\rvert \leqslant 1$ $f = 0$, $\lvert\zeta\rvert > 1$	1/2	1/3	1/4	1.300
Trapezoidal, $f = 1$, $\lvert\zeta\rvert \leqslant 1$ $f = (a-\zeta)/(a-1)$, $1 < \lvert\zeta\rvert \leqslant a$ $f = 0$, $\lvert\zeta\rvert > a$	1–1/2	1–1/3	1–1/4	1–1.3
Top hat, $f = 1$, $\lvert\zeta\rvert \leqslant 1$ $f = 0$, $\lvert\zeta\rvert > 1$	1	1	1	1
Parabolic, $f = 1-\zeta^2$, $\lvert\zeta\rvert \leqslant 1$ $f = 0$, $\lvert\zeta\rvert > 1$	2/3	8/15	16/35	1.173
Gaussian, $f = \exp(-\zeta^2)$	$\pi^{1/2}$	$(\pi/2)^{1/2}$	$(\pi/3)^{1/2}$	0.729
Exact, $f = 1-\tanh^2\zeta$	2	4/3	16/15	0.693

tudinal location of the nozzle relative to the virtual origin.

The classical similarity solution to the same problem [5] (also pp. 291 and 292 of ref. [3]) covers more territory, in the sense that it produces not only the equivalent of equations (7) and (8) but also a solution for the shape of the u-profile

$$f = 1 - \tanh^2 \zeta. \tag{11}$$

This 'exact' solution requires a hypothesis of its own, namely the use of the mixing-length model

$$\varepsilon_M = \frac{u_c x}{4\gamma^2} \tag{12}$$

in which γ is an empirical constant the recommended value of which is [6]

$$\gamma \cong 7.67. \tag{13}$$

In place of equation (8), for example, Görtler's similarity solution (11) has

$$\tilde{u}_c = \left(\frac{4\gamma}{3}\right)^{1/2} \tilde{x}^{-1/2}. \tag{14}$$

Comparing this with equation (8), and using equations (6), (11) and (13), we conclude that the proper empirical value of the entrainment coefficient used in the integral analysis is

$$\alpha_e \cong 0.0367. \tag{15}$$

This introductory analysis shows that the entrainment hypothesis is the integral-solution equivalent of the mixing length model used in the earliest similarity solutions of free turbulent flows. Both approaches lead to the conclusion that the time-averaged flow region is wedge-shaped (i.e. that D is proportional to x, equation (9)), and that the centerline velocity decreases as $x^{-1/2}$. The analysis is based on only two equations (mass, momentum) and one act of empiricism represented by the chosen value of α.

Critical to defining the objective of the present study was the observation that the preceding analysis has absolutely no use for thermodynamic considerations such as the first law (energy equation) and the second law. Indeed, the flows that are being subjected to mass-and-momentum-only analysis are sometimes referred to as 'isothermal'. The objective of the work described next is to provide a more complete view of the flow, this time by taking into account also the first and second laws of thermodynamics.

THE FIRST LAW OF THERMODYNAMICS

Consider the first-law statement for the steady jet flow through the control volume of thickness dx, defined by the two planes drawn normal to the x-axis in Fig. 1

$$\frac{d}{dx}\int_{-\infty}^{\infty} \rho u\left(h + \frac{u^2}{2}\right) dy = \left[h_\infty + \frac{(-v_\infty)^2}{2}\right] \frac{d}{dx}\int_{-\infty}^{\infty} \rho u \, dy. \tag{16}$$

The left-hand side of this equation—or the 'LHS' arrow on Fig. 1—represents the net increase in the longitudinal flow of energy through the jet. The right-hand side ('RHS') accounts for the energy brought into the jet region by the entrainment process. On both sides of the equation, the local specific energy is the sum of the local time averaged enthalpy (h) and the local kinetic energy of the time averaged flow ($u^2/2$). The kinetic energy contributions associated with time-averaged products of fluctuation velocity components are assumed negligible relative to the kinetic energy of the main stream ($u^2/2$).

A useful alternative to equation (16) is

$$\frac{d}{dx}\int_{-\infty}^{\infty} \rho u\left(h - h_\infty + \frac{u^2}{2}\right) dy = \frac{(-v_\infty)^2}{2} \frac{d}{dx}\int_{-\infty}^{\infty} \rho u \, dy \tag{17}$$

in which we can set $h - h_\infty = c_p(T - T_\infty)$, because the pressure is uniform throughout the jet flow region. If the fluid behaves as an incompressible liquid, then $h - h_\infty = c(T - T_\infty)$, in which c is the lone specific heat of the liquid. In what follows, c_p (or c) is treated as a constant, in other words, it is assumed that the temperature excursion $T - T_\infty$ is sufficiently small when compared with the absolute temperature T_∞.

Finally, for simplicity it is assumed that the time-averaged temperature profile has the same shape and transversal length scale as the longitudinal velocity profile

$$T - T_\infty = (T_c - T_\infty) f(\zeta). \tag{18}$$

In this equation, $T_c(x)$ is the temperature distribution along the jet centerline.

Method 1

There are two ways of pursuing the energy conservation requirement embodied in equation (17). The first is the 'consistent' approach of applying the entrainment hypothesis (7) one more time, in order to evaluate the leading factor on the right-hand side of equation (17). The end result of the ensuing analysis is an expression for the centerline temperature difference

$$\Delta\tilde{T}_c = \frac{I_3 + \alpha^2 I_1}{I_2^2}\left[\left(\frac{I_1}{4\alpha\tilde{x}}\right)^{1/2} - \frac{I_1}{4\alpha\tilde{x}}\right] \tag{19}$$

in which $\Delta\tilde{T}_c$ is dimensionless

$$\Delta\tilde{T}_c = \frac{c_p}{u_0^2/2}(T_c - T_\infty) \tag{20}$$

and I_3 is a third constant dictated by the profile shape function (Table 1)

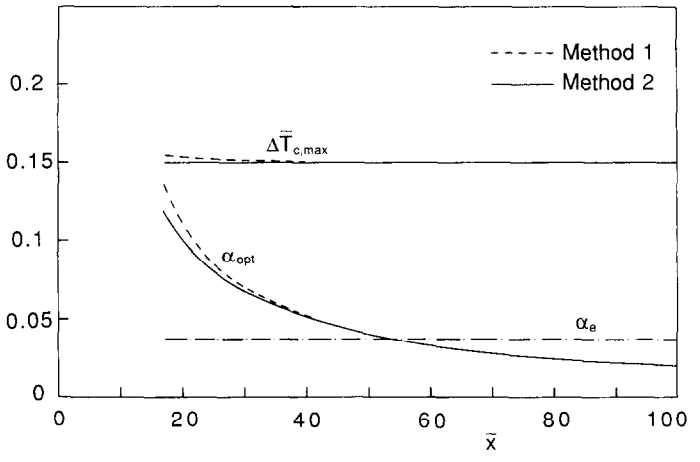

FIG. 2. The optimum entrainment coefficient for maximum temperature rise on the jet centerline.

$$I_3 = \int_{-\infty}^{\infty} f^3 \, d\zeta. \tag{21}$$

Equation (19) was obtained by integrating equation (17) once in x, and making the statement that the jet fluid is isothermal in the nozzle cross-section, i.e. $\Delta\tilde{T}_c = 0$ at $\tilde{D} = 1$.

The relationship between temperature rise ($\Delta\tilde{T}_c$), entrainment coefficient (α), and longitudinal position ($\tilde{x}$) is described by equation (19). Most interesting is that at a fixed longitudinal position the centerline temperature reaches a maximum value ($\Delta\tilde{T}_{c,max}$) for a special value of the entrainment coefficient (α_{opt}). These values can be determined by maximizing the right-hand side of equation (19) numerically: the results are indicated by the dash curves in Fig. 2. This figure was constructed using the $I_{1,2,3}$ constants of the exact jet profile (Table 1).

The maximum centerline temperature is practically independent of longitudinal position, $\Delta\tilde{T}_{c,max} \cong 0.15$, while α_{opt} decreases monotonically as $\tilde{x}$ increases. It is important to note that α_{opt} is of the same order of magnitude as the empirical entrainment coefficient ($\alpha_e = 0.0367$). This observation is particularly valid at longitudinal positions greater than several slit widths, i.e. in the self-similar region of the jet, which is responsible for the measurement of α_e.

Method 2

With regard to the energy content of the entrained flow, it can also be argued that since the fluid reservoir is at rest, the kinetic energy part $(-v_x)^2/2$ should be zero in equations (16) and (17). A thermodynamicist not familiar with the entrainment hypothesis (7) will most likely follow this approach. In this case, the centerline temperature distribution that replaces equation (19) is

$$\Delta\tilde{T}_c = \frac{I_3}{I_2^2}\left[\left(\frac{I_1}{4\alpha\tilde{x}}\right)^{1/2} - \frac{I_1}{4\alpha\tilde{x}}\right]. \tag{22}$$

This time, the optimum entrainment coefficient that maximizes the centerline temperature at any given $\tilde{x}$ can be determined in closed form

$$\alpha_{opt} = \frac{I_1}{\tilde{x}} \tag{23}$$

$$\Delta\tilde{T}_{c,max} = \frac{I_3}{4I_2^2}. \tag{24}$$

These results are represented by the solid curves in Fig. 2, again, by using the $I_{1,2,3}$ constants of the exact jet profile. There is little difference between the present results and those derived based on Method 1. In fact, the two methods lead to practically the same α_{opt} and $\Delta\tilde{T}_{c,max}$ values in the downstream region beyond several slit widths, reinforcing the conclusion that the optimum α that maximizes $\Delta\tilde{T}_c$ is of the same order of magnitude as the empirical value α_e.

This conclusion is backed further by Fig. 3, which shows the actual centerline temperature of the jet, as a function of $\tilde{x}$. The single curve in this figure represents the superposition of equations (19) and (22), in which $\alpha = \alpha_e$ and $I_{1,2,3}$ are the constants listed for the exact profile in Table 1. In this case, the nozzle is located at $\tilde{x} = 13.6$ away from the virtual origin, and the theoretical maximum centerline temperature is $\Delta\tilde{T}_{c,max} = 0.15$, cf. equation (24).

Figure 3 shows that the actual centerline temperature of the jet is nearly the same as $\Delta\tilde{T}_{c,max}$ for a long section of the jet, beyond some distance downstream from the nozzle. This observation has its explanation in the lower part of Fig. 2, in which the theoretical coefficient α_{opt} was found to be equal to, or comparable with the empirical value α_e. In conclusion, the introduction of an empirical parameter (α) in the pure fluid mechanics treatment of the jet problem is accompanied by an extremum ($\Delta\tilde{T}_{c,max}$) in the first-law analysis of the same flow.

THE SECOND LAW OF THERMODYNAMICS

The preceding conclusions were based on the first-law analysis of the jet region. With reference to the

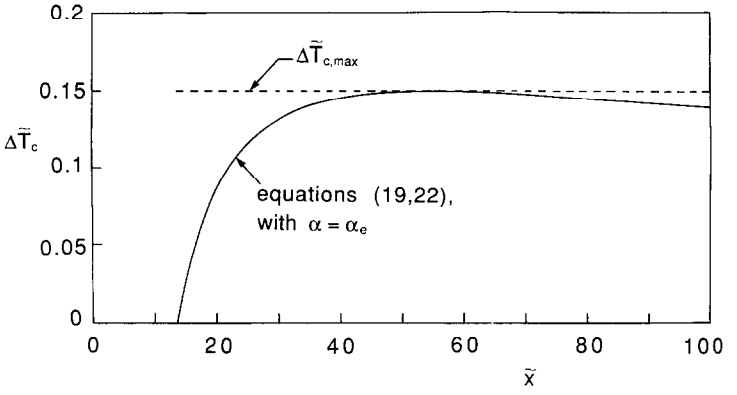

FIG. 3. The effect of $\tilde{x}$ on the actual centerline temperature distribution ($\alpha = \alpha_e$).

control volume of thickness dx defined in Fig. 1, the second law states that the rate of entropy generation is non-negative

$$\frac{dS_{gen}}{dx} = \frac{d}{dx}\int_{-\infty}^{\infty} \rho u s \, dy - s_\infty \frac{d}{dx}\int_{-\infty}^{\infty} \rho u \, dy \geqslant 0. \tag{25}$$

The two terms that appear on the right-hand side of equation (25) are associated respectively with the 'LHS' and 'RHS' arrows drawn on Fig. 1.

When the two integrals of equation (25) are combined, the local time-averaged entropy change $(s - s_\infty)$ appears as a factor in the integrand. This group can be replaced approximately by

$$s - s_\infty \cong \frac{c_p}{T_\infty}(T - T_\infty) \tag{26}$$

because the pressure is uniform and the temperature rise is negligible relative to the absolute temperature (see the discussion under equation (17)). Assuming further that the temperature and velocity profiles are described by the same $f(\zeta)$, equation (18), the entropy generation rate (25) can be expressed as

$$\frac{d\tilde{S}_{gen}}{d\tilde{x}} = \frac{d}{d\tilde{x}}(I_2 \tilde{u}_c \tilde{D} \Delta\tilde{T}_c) \tag{27}$$

where

$$\tilde{S}_{gen} = \frac{S_{gen}}{\rho u_0^3 D_0 / 2T_\infty}. \tag{28}$$

Integrating equation (27) from the nozzle (where $\Delta\tilde{T}_c = 0$) to any $\tilde{x}$ situated downstream from the nozzle yields

$$\tilde{S}_{gen} = I_2 \tilde{u}_c \tilde{D} \Delta\tilde{T}_c. \tag{29}$$

Note that the physical (dimensional) entropy generation rate S_{gen} listed in equation (28) represents the rate of entropy generation in the jet section (finite control volume) contained between the plane of the nozzle and a particular constant-x plane situated downstream.

Equation (29) can be combined with the results obtained previously for $\tilde{u}_c$, $\tilde{D}$ and $\Delta\tilde{T}_c$, in order to determine the ways in which α, $\tilde{x}$ and the profile shape $f(\zeta)$ influence the rate of entropy generation. In the case of $\Delta\tilde{T}_c$, we have a choice between equations (19)

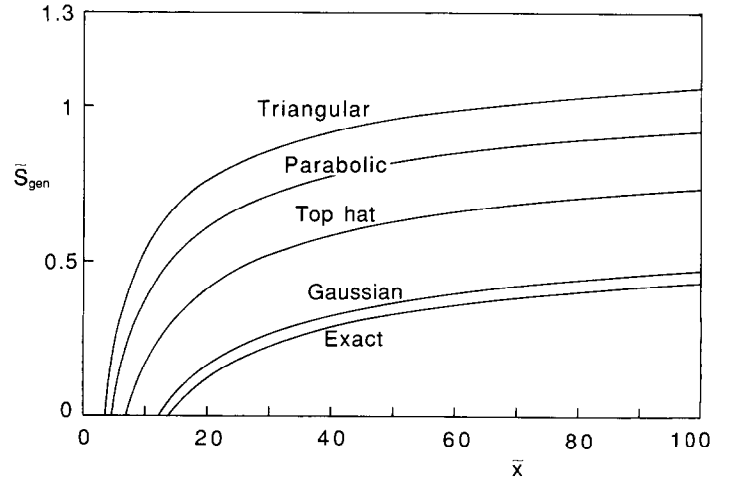

FIG. 4. The effect of $\tilde{x}$ and profile shape on the total entropy generation rate ($\alpha = \alpha_e$).

and (22); the following expression is based on equation (22):

$$\tilde{S}_{\text{gen}} = \frac{I_3}{I_2^{3/2}}\left[1-\left(\frac{I_1}{4\alpha\tilde{x}}\right)^{1/2}\right] \tag{30}$$

and shows that $\tilde{S}_{\text{gen}}$ increases monotonically as α and $\tilde{x}$ increase. The $\tilde{x}$ dependence is illustrated in Fig. 4, which was drawn using the empirical entrainment coefficient, $\alpha = \alpha_e$. The entropy generation rate approaches a ceiling value $\tilde{S}_{\text{gen,max}}$ as the length of the jet becomes considerably greater than the distance from the virtual origin to the nozzle, $\tilde{x} \gg I_1/4\alpha$

$$\tilde{S}_{\text{gen,max}} = \frac{I_3}{I_2^{3/2}}. \tag{31}$$

Figure 4 and equation (31) show that the entropy generation rate distribution depends on the shape of the velocity and temperature profile, $f(\zeta)$. Recall that in the integral method employed throughout this paper we have the freedom to select any profile shape that is 'reasonable' (i.e. one that satisfies the conditions $f(0) = 1$, $f'(0) = 0$, $f(\pm\infty) = 0$). In the case of the jet of Fig. 1 we have also the luxury to know the 'exact' profile supplied by Görtler's solution, equation (11). Table 1 shows a compilation of reasonable profiles, ranging from the piecewise linear (top hat, trapezoidal, triangular) to the bell-shaped profiles that are being used routinely in integral jet analyses. The table shows that the group $I_3/I_2^{3/2} = \tilde{S}_{\text{gen,max}}$ decreases as the shape $f(\zeta)$ becomes more reasonable, that is, more like the shape revealed by time-averaged measurements. The smallest value of the group $I_3/I_2^{3/2}$ corresponds to the exact profile (11). The Gaussian profile, which is often used to correlate jet velocity and temperature measurements, yields a $\tilde{S}_{\text{gen,max}}$ value that is only 5% greater than that of the exact profile.

On the basis of the evidence assembled in Table 1, it can be argued that the proper velocity and temperature profile shape is the one that minimizes the total entropy generation rate of a jet of finite length. Other reasonable profile shapes can be tried and added to Table 1, in order to strengthen or refute this argument.

CONCLUSIONS

The objective of this study has been to investigate the thermodynamic characteristics of a traditional 'isothermal' forced flow configuration, that is, to complete the missing part of the traditional pure-fluid-mechanics treatment. Using the two-dimensional turbulent jet as an example, we saw that the empirical elements of the traditional integral analysis (the coefficient α, and the profile $f(\zeta)$) have interesting extrema as counterparts in the first-law and second-law analyses of the same flow:

(1) The maximum temperature rise at a fixed $\tilde{x}$ on the jet centerline corresponds to a certain value of the entrainment coefficient, which is comparable with the empirical value α_e (Figs. 2 and 3).

(2) The observed shape of the velocity and temperature profiles corresponds to the smallest total entropy generation rate (Table 1, Fig. 4).

The present study is important for two reasons. First, it unveils the thermodynamic picture that is being overlooked entirely by a pure-fluid-mechanics analysis, which often relies on empiricism in order to produce a solution. This comment is not offered as criticism of the classical fluid mechanics work, rather, it is a thought that future analysts may benefit from knowing precisely what is being overlooked when a new problem is attacked by relying on the traditional method.

The second reason why I found the present subject interesting enough to pursue it, is the correspondence that appears to exist between the empirical aspect to the pure fluid mechanics treatment, and the temperature and entropy generation extrema of the thermodynamic analysis. This correspondence deserves further study, for example, by focusing on other basic flow configurations.

Acknowledgement—The research reported in this paper was supported by the National Science Foundation through Grant No. CBT-8711369.

REFERENCES

1. R. J. Krane, A second law analysis of the optimum design and operation of thermal energy storage systems, *Int. J. Heat Mass Transfer* **30**, 43–57 (1987).
2. R. B. Evans and M. R. von Spakovsky, Two principles of differential second law analysis for heat exchanger design. In *Approaches to the Design and Optimization of Thermal Systems*, AES Vol. 7. ASME, New York (1988).
3. A. Bejan, *Convection Heat Transfer*. Wiley, New York (1984).
4. B. Morton, G. I. Taylor and J. S. Turner, Turbulent gravitational convection from maintained and instantaneous sources, *Proc. R. Soc. London* **A234**, 1–23 (1956).
5. H. Görtler, Berechnung von Aufgaben der freien Turbulenz auf Grund eines neuen Näherungsansatzes, *Z. Angew. Math. Mech.* **22**, 244–254 (1942).
6. H. Reichardt, Gesetzmässigkeiten der freien Turbulenz, *VDI ForschHft* 414 (1951).

THERMODYNAMIQUE D'UN ECOULEMENT ISOTHERME: LE JET TURBULENT BIDIMENSIONNEL

Résumé—Cette étude illustre l'information thermodynamique qui est habituellement négligée dans la mécanique des fluides classiques. L'analyse intégrale d'un jet bidimensionnel est utilisée comme exemple. On montre que même quand la différence de température entre le nez de la tuyère et le fluide ambiant est nulle, le jet lui-même n'est pas isotherme. A toute position le long du jet, l'élévation de température est maximale quand le coefficient d'entrainement prend une valeur comparable avec la valeur déterminée expérimentalement. Il apparait que la forme naturelle des profils de vitesse et de température du jet est celle qui minimise le taux de création d'entropie. Cette étude suggère qu'il existe une relation importante entre les composantes empiriques du traitement de la mécanique des fluides classiques et les extrema de température et d'entropie dégagés par la thermodynamique.

THERMODYNAMIK EINER "ISOTHERMEN" STRÖMUNG: DER ZWEIDIMENSIONALE TURBULENTE STRAHL

Zusammenfassung—Die vorliegende Arbeit veranschaulicht die thermodynamische Information, welche üblicherweise bei einer Untersuchung der Strömungsmechanik reiner Stoffe übersehen wird. Als Beispiel wird die integrale Berechnung eines zweidimensionalen turbulenten Strahls verwendet. Dabei zeigt sich, daß, selbst wenn keine Temperaturdifferenz zwischen dem Fluid in der Düse und demjenigen im Reservoir besteht, die Strahlströmung nicht isotherm ist. An jeder Stelle des Strahls erreicht der Temperaturanstieg ein Maximum, wenn der Entrainment-Koeffizient einen Wert annimmt, der dem experimentell ermittelten vergleichbar ist. Außerdem stellt sich heraus, daß die natürliche Form der Geschwindigkeits- und Temperaturprofile des Strahls einem Minimum der Gesamtentropie-Erzeugungsrate entspricht. Als Schlußfolgerung ergibt sich, daß zwischen den empirischen Komponenten der integralen Behandlung der Fluidmechanik und den Extrema der Temperatur und der Entropieerzeugung ein wichtiger Zusammenhang besteht.

ТЕРМОДИНАМИКА "ИЗОТЕРМИЧЕСКОГО" ТЕЧЕНИЯ: ДВУМЕРНАЯ ТУРБУЛЕНТНАЯ СТРУЯ

Аннотация—Приводятся данные по термодинамике, обычно не учитываемые в теоретической гидродинамике. В качестве примера используется интегральный анализ двумерной турбулентной струи. Показано, что даже при нулевой разности температур между жидкостью в сопле и резервуаре область струйного течения является неизотермической. В каждой точке вдоль струи рост температуры становится максимальным, когда коэффициент переноса принимает значение, сопоставимое с экспериментальным. Кроме того, оказывается, что естественная форма скоростного и температурного профилей струи минимизирует полую скорость производства энтропии. Предполагается, что существует связь между эмпирическими компонентами интегрального анализа чистой гидродинамики и экстремумами температуры и производства энтропии, полученными при термодинамическом анализе.